Defence Science Journal, Vol. 74, No. 3, May 2024, pp. 321-328, DOI : 10.14429/dsj.74.19886


# Elastic Damage-Healing Model Coupling Secondary Damage Variable for Self-Healing Materials

Harini Subramanian and Shantanu S. Mulay*

*Department of Aerospace Engineering, Indian Institute of Technology Madras, Chennai - 600 036, India*

**E-mail: ssmulay@smail.iitm.ac.in*

**ABSTRACT**

A one-dimensional constitutive model, based on the principles of continuum damage mechanics, is developed for capturing healing in certain materials during unloading and rest periods. A secondary damage variable $D_l^s$ is defined to address the drawback of existing models for damage and healing in capturing the complete material failure. An energy-based damage evolution function is adopted for primary and secondary damage variables, and phenomenological healing evolution is defined. The proposed implicit elastic damage-healing model is implemented by the return-mapping technique, and the model response is demonstrated for different loading histories.

**Keywords:** Damage-healing model; Self-healing materials

## 1. INTRODUCTION

Self-healing is a biologically inspired phenomenon in materials to reverse the degradation or damage, introducing healing and thus delaying material failure for example, asphalt[1]. Self-healing materials, such as self-healing polymers and surface coatings, are commercially manufactured (to reduce repair costs). Cross-linked epoxidized polysulphide polymer is healed at room temperature by trin-butylphosphine with repeated restoration of the tensile strength[2], and intrinsic self-healing is also obtained in synthetic rubbers[3].

The self-healing constitutive model is developed for materials that can heal in the unloading and rest periods, where wetting of damaged surfaces results in partial strength recovery[4]. Continuum damage mechanics (CDM)-based damage-healing models are developed in the literature, where the combined effect of damage and healing is quantified by a variable capturing the effective damage in the material as $\phi = D_g(1-h_l)$ ($\phi$=0 represents no damage and $\phi$=1 represents fully damage)[4-6]. CDM-based damage-healing models have also been proposed using a consistent thermodynamic framework for glassy polymers and polymer matrix composites[7-8]. The plastic, viscoelastic, or visco-plastic response of the material is modelled by the appropriate definition of the Helmholtz free energy function [5, 9-12].

Cohesive zone-based approaches have also been developed to study crack propagation in a self-healing material, exploring different fracture properties of the healing agent compared to the parent material (extrinsic healing)[13]. Micromechanical models for healing have also been proposed to study the influence of healing capsule properties on the mechanical response of micro-capsule-enabled self-healing concrete[14].

This $\phi$ cannot capture the complete material failure (drawback), as it does not track damage occurring in a healed material. This limitation is overcome by proposing a secondary damage variable $D_l^s$ capturing degradation in a healed material[10-12], where $\phi_{eff} = D_g[1 - h_l(1 - D_l^s)]$ is proposed. The novelty of the present work is the development of an elastic damage-healing model with an implicit energy-based damage evolution function such that a threshold energy governs damage initiation. Damage occurs when applied loading exceeds threshold energy, while healing occurs while unloading or in a rest state when strain is below a healing threshold strain. The damaged surfaces are closer to each other below the threshold strain for bond reformation and recovery of material strength. The algorithmic tangent modulus is obtained for different loading and unloading stages, and the influence of healing observed as a recovery of stiffness (tangent modulus) is demonstrated.

## 2. DAMAGE MECHANICS FOR SELF-HEALING

CDM is modified (known as continuum damage-healing mechanics (CDHM)) to account for the healing of damage by defining a healing configuration (analogous to the effective configuration in CDM), thus retaining only undamaged and damaged-healed materials. Isotropic damage and healing variables are defined to quantify the damaged and healed areas in the loaded material. The *global* damage and *local* healing variables are defined as [10-12, 15]

$$D_g = \frac{dA^D}{dA}, h_l = \frac{dA_h^D}{dA^D} \tag{1}$$

Received : 12 February 2024, Revised : 18 February 2024
Accepted : 27 February 2024, Online published : 10 May 2024

Where, $dA^D$ is the cross-sectional area undergoing damage, $dA$ is the area of unloaded virgin material, and $dA_h^D$ is the healing in the damaged area. The secondary damage variable for healed material damage is defined as[10-12]

$$D_l^s = \frac{(dA_h^D)^D}{dA_h^D} \tag{2}$$

where, $(dA_h^D)^D$ is the damaged-healed area undergoing re-damage. The stresses in the actual ($\sigma$) and fictitious healing ($\tilde{\tilde{\sigma}}$) configurations are related as (the mechanical equivalence principle)

$$\tilde{\tilde{\sigma}} = \frac{\sigma}{1 - D_g[1 - h_l(1 - D_l^s)]} \tag{3}$$

The *elastic strain* equivalence hypothesis (current configuration strain $\epsilon^e$ equals healing configuration strain $\tilde{\tilde{\epsilon}}^e$) is used to obtain stiffness in the current configuration (1D) as[10-12,15]

$$\epsilon^e = \tilde{\tilde{\epsilon}}^e \Rightarrow E(\phi_{eff}) = (1 - \phi_{eff})E_0 \tag{4}$$

where, $E_0$ and $E(\phi_{eff})$ are stiffness values in the original and damaged materials, respectively. The stress-strain relation in the current configuration is derived using Eqns. (3) and (4) as

$$\tilde{\tilde{\sigma}} = E_0\tilde{\tilde{\epsilon}}^e \Rightarrow \sigma = E_0(1 - \phi_{eff})\epsilon^e \tag{5}$$

## 3. ELASTIC DAMAGE-HEALING MODEL

An elastic damage-healing (EDH) model, capturing the healing in *unloading* and *rest* periods, is presented. The damage evolution (primary and secondary) is governed by an energy-based criterion. The primary damage evolution function is given as[16]

$$f^{D_g} = (1 - D_g)^{m(D_g)} Y^{D_g} - W_0 e^{(-\beta D_g(1-D_g))} > 0 \tag{6}$$

where, $Y^{D_g}$ is the energy release rate (J/m$^3$) for damage in virgin material, $m(D_g)$ is the exponent in damage evolution function calibrated for the material, $W_0$ is the threshold energy beyond which damage initiates in virgin material, and $e^{(-\beta D_g(1-D_g))}$ is the exponential function controlling the degradation of $W_0$ ($\beta$ is a material constant). The exponent function $m(D_g) = m_1(1 - D_g)^{m_2} + m_3$ is obtained by finding the scalar constants $m_1$, $m_2$ and $m_3$ for the material subject to the conditions: $m_1 + m_3 > 2$ and $m_3 < 2$, for correctly capturing the hardening and softening responses of the material's $\sigma$-$\epsilon$ curve. These functions take the following form in 1D damage-healing mechanics as

$$W_0 = \frac{1}{2}E\epsilon_0^2, \qquad Y^{D_g}(\epsilon, h_l, D_l^s) = \frac{1}{2}[1 - h_l(1 - D_l^s)]E\epsilon^2 \tag{7}$$

where, $\epsilon_0$ is the threshold strain governing damage initiation. Energy-based damage evolution is used in the present work for two reasons. **(1)**The elastic part of strain energy (stored in the spring part of mechanical analogue considered for a said material), for many materials, like visco-elasticity, drives the damage evolution. **(2)** The threshold energy, in many materials, also increases as damage progresses (strain hardening), and it also decreases beyond a certain damage value (strain softening). This feature is well captured in the present Eq. (6), as the damage progresses from $D_g \approx 0$ to $D_g \approx 1$. A healing increment making $h_l$ a function of prior $D_g$ and $h_l$ is defined as[4]

$$\dot{h}_l = \beta_h[(1 - D_g)(1 - h_l)]^p \tag{8}$$

where, $\beta_h$ is dependent on material viscosity and controls the healing rate, whereas $p$ is a constant determined by calibration using experimental data. An initiation condition for healing is postulated as $f^{h_l} = \epsilon_{th}^{h_l} - \epsilon_{eff} \le 0$, where $f^{h_l}$ is the surface driving healing evolution such that healing evolves when the effective strain ($\epsilon_{eff}$) is below the healing threshold strain $(\epsilon_{th}^{h_l})$ (Note: $\epsilon_{eff} = \epsilon$ for 1D case). The evolution of $D_l^s$ is considered similar to $D_g$ as

$$f^{D_l^s} = (1 - D_l^s)^{m(D_l^s)} Y^{D_l^s} - W_0 e^{(-\beta D_l^s(1-D_l^s))} > 0 \tag{9}$$

where, $Y^{D_l^s}$ is the energy release rate for secondary damage (J/m$^3$), $m(D_l^s)$ is a parameter similar to $m(D_g)$, $W_0$ is the energy threshold for initiation of damage in healed material, and $e^{(-\beta D_l^s(1-D_l^s))}$ is the function governing its degradation just as in the case of primary damage. The energy release rate for damage in healed material 1-D CDHM is given as [10-12]

$$Y^{D_l^s}(\epsilon, D_g, h_l) = \frac{1}{2}D_g h_l E\epsilon^2 \tag{10}$$

## 4. ALGORITHMIC IMPLEMENTATION OF ELASTIC DAMAGE-HEALING MODEL

The algorithm of the proposed damage-healing model is shown in Box 5.1. The algorithmic tangent modulus expressions, which can be used while solving boundary value problems, are detailed in this section.

### 4.1 Tangent Modulus

The tangent modulus in algorithmic form relating $\Delta\sigma$ and $\Delta\epsilon$ is obtained using Eqn. (5) as

$$E_{j+1}^T = \frac{\partial\sigma_{j+1}}{\partial\epsilon_{j+1}} = E_0(1 - (\phi_{eff})_{j+1}) - \frac{\partial(\phi_{eff})_{j+1}}{\partial\epsilon_{j+1}}E_0\epsilon_{j+1} \tag{11}$$

where $[\partial(\phi_{eff})_{j+1}/\partial\epsilon_{j+1}]$ is given as

$$\frac{\partial(\phi_{eff})_{j+1}}{\partial\epsilon_{j+1}} = \frac{\partial(D_g)_{j+1}}{\partial\epsilon_{j+1}}[1 - (h_l)_{j+1}(1 - (D_l^s)_{j+1})] - \frac{\partial(h_l)_{j+1}}{\partial\epsilon_{j+1}}(D_g)_{j+1}(1 - (D_l^s)_{j+1}) + \frac{\partial(D_l^s)_{j+1}}{\partial\epsilon_{j+1}}(D_g)_{j+1}(h_l)_{j+1} \tag{12}$$

The $[\partial(D_g)_{j+1}/\partial\epsilon_{j+1}]$ is obtained by $(f^{D_g})_{j+1} = 0$ from Eqn. (6) as

$$\Bigg[\underbrace{\frac{\partial m(D_g)_{j+1}}{\partial(D_g)_{j+1}}\log(1 - (D_g)_{j+1}) - \frac{m(D_g)_{j+1}}{(1 - (D_g)_{j+1})} + \beta(1 - 2(D_g)_{j+1})}_{DR}\Bigg] \frac{\partial(D_g)_{j+1}}{\partial\epsilon_{j+1}} + \frac{1}{(Y^{D_g})_{j+1}}\left[\frac{\partial(Y^{D_g})_{j+1}}{\partial\epsilon_{j+1}} + \frac{\partial(Y^{D_g})_{j+1}}{\partial(h_l)_{j+1}}\frac{\partial(h_l)_{j+1}}{\partial\epsilon_{j+1}} + \frac{\partial(Y^{D_g})_{j+1}}{\partial(D_l^s)_{j+1}}\frac{\partial(D_l^s)_{j+1}}{\partial\epsilon_{j+1}}\right] = 0 \tag{13}$$

The $[\partial(D_l^s)_{j+1}/\partial\epsilon_{j+1}]$ is obtained by $(f^{D_l^s})_{j+1} = 0$ from Eqn. (7) as

$$\Bigg[\underbrace{\frac{\partial m(D_l^s)_{j+1}}{\partial(D_l^s)_{j+1}}log(1 - (D_l^s)_{j+1}) - \frac{m(D_l^s)_{j+1}}{(1 - (D_l^s)_{j+1})} + \beta(1 - 2(D_l^s)_{j+1})}_{DR_2}\Bigg] \frac{\partial(D_l^s)_{j+1}}{\partial\epsilon_{j+1}} + \frac{1}{(Y^{D_l^s})_{j+1}}$$

$$\left[\frac{\partial(Y^{D_l^s})_{j+1}}{\partial\epsilon_{j+1}} + \frac{\partial(Y^{D_l^s})_{j+1}}{\partial(h_l)_{j+1}}\frac{\partial(h_l)_{j+1}}{\partial\epsilon_{j+1}} + \frac{\partial(Y^{D_l^s})_{j+1}}{\partial(D_g)_{j+1}}\frac{\partial(D_g)_{j+1}}{\partial\epsilon_{j+1}}\right] = 0 \quad (14)$$

The subscript ($j$ + 1) is not used in the subsequent equations for simplification.

Different internal / state variables evolve along the path of the stress-strain plot, resulting in different tangent moduli expressions as follows.

**Case 1:** $D_g$ alone evolves without any prior healing ($h_l = D_l^s = 0$), Eqn. (13) gives

$$\frac{\partial D_g}{\partial\epsilon} = \frac{-\frac{1}{Y^{D_g}}\left(\frac{\partial Y^{D_g}}{\partial\epsilon}\right)}{DR} \quad (15)$$

The tangent modulus is given by substituting Eqn. (15) in Eqns. (12) and (11) to get

$$E^T = E_0(1-\phi_{eff}) + \frac{\frac{1}{Y^{D_g}}\left(\frac{\partial Y^{D_g}}{\partial\epsilon}\right)}{DR}E_0[1-(h_l)(1-(D_l^s))]\epsilon \quad (16)$$

**Case 2:** $D_g$ alone evolves ($h_l \neq 0$ *and* $D_l^s = 0$), $h_l$ is updated keeping *healed* area constant

$$dA_h^D = \text{constant} \Rightarrow h_g = h_l D_g = \text{constant} \Rightarrow$$

$$\frac{\partial(h_l)}{\partial\epsilon} = -\underbrace{\frac{(h_l)_z(D_g)_z}{(D_g)^2}}_{A}\frac{\partial D_g}{\partial\epsilon} \quad (17)$$

Eqn. (13) is simplified by $D_g \neq 0, h_l \neq 0$, and $\dot{D}_l^s = 0$ to get

$$\left[\frac{\partial m(D_g)}{\partial D_g}\log(1-D_g) - \frac{m(D_g)}{(1-D_g)} + \beta(1-2D_g)\right]$$
$$\frac{\partial D_g}{\partial\epsilon} + \frac{1}{Y^{D_g}}\left[\frac{\partial Y^{D_g}}{\partial h_l}\frac{\partial h_l}{\partial\epsilon}\right] = \frac{-1}{Y^{D_g}}\frac{\partial Y^{D_g}}{\partial\epsilon} \quad (18)$$

Eqn. (17) and (18) are solved together to obtain $\partial D_g/\partial\epsilon$ and $\partial h_l/\partial\epsilon$ as

$$\frac{\partial D_g}{\partial\epsilon} = \frac{\frac{-1}{Y^{D_g}}\frac{\partial Y^{D_g}}{\partial\epsilon}}{DR - \frac{A}{Y^{D_g}}\left[\frac{\partial Y^{D_g}}{\partial h_l}\right]}, \quad \frac{\partial h_l}{\partial\epsilon} = \frac{\frac{A}{Y^{D_g}}\frac{\partial Y^{D_g}}{\partial\epsilon}}{DR - \frac{A}{Y^{D_g}}\left[\frac{\partial Y^{D_g}}{\partial h_l}\right]} \quad (19)$$

The tangent modulus is obtained using Eqns. (11), (12), and (19) as

$$E^T = E_0(1-\phi_{eff}) + \left[\frac{\frac{-1}{Y^{D_g}}\frac{\partial Y^{D_g}}{\partial\epsilon}}{DR - \frac{A}{Y^{D_g}}\left[\frac{\partial Y^{D_g}}{\partial h_l}\right]}\right]E_0[1-h_l(1-D_l^s)]\epsilon - \left[\frac{\frac{A}{Y^{D_g}}\frac{\partial Y^{D_g}}{\partial\epsilon}}{DR - \frac{A}{Y^{D_g}}\left[\frac{\partial Y^{D_g}}{\partial h_l}\right]}\right]E_0 D_g(1-D_l^s)\epsilon \quad (20)$$

**Case 3:** $D_g$ and $D_l^s$ evolve, and $h_l$ is updated as Case 2 ($h_l \neq 0$). The Eqs. (13), (14), and (17) are solved to obtain

**Box 5.1: 1D local EDH stress update return mapping equations**

Stress update and computation of primary damage, healing, and secondary damage for a given strain increment $\Delta\varepsilon_{n+1}$

1. **Estimation of** $(D_g)_{n+1}$, $(h_l)_{n+1}$, **and** $(D_l^s)_{n+1}$
   (a) **Loading,** $(f^{D_g})^{tr}_{n+1} > 0$ **and no healing:**

   $(h_l)_{n+1} = 0, \quad (D_l^s)_{n+1} = 0, \quad (f^{D_g})_{n+1} = [1-(D_g)_{n+1}]^{m((D_g)_{n+1})}(Y^{D_g})_{n+1} - W_0\exp[-\beta(D_g)_{n+1}(1-(D_g)_{n+1})] = 0$

   (b) **Loading,** $(f^{D_g})^{tr}_{n+1} > 0$ **and** $(f^{D_l^s})^{tr}_{n+1} > 0$ **with prior healing:**

   $(f^{D_g})_{n+1} = [1-(D_g)_{n+1}]^{m((D_g)_{n+1})}(Y^{D_g})_{n+1} - W_0\exp[-\beta(D_g)_{n+1}(1-(D_g)_{n+1})] = 0$

   $(h_l)_{n+1} = \frac{(h_l)_n(D_g)_n}{(D_g)_{n+1}}$

   $(f^{D_l^s})_{n+1} = \left[1-(D_l^s)_{n+1}\right]^{m((D_l^s)_{n+1})}(Y^{D_l^s})_{n+1} - W_0\exp\left[-\beta(D_l^s)_{n+1}\left(1-(D_l^s)_{n+1}\right)\right] = 0$

   (c) **Loading,** $(f^{D_g})^{tr}_{n+1} < 0$ **and** $(f^{D_l^s})^{tr}_{n+1} > 0$ **with prior healing:**

   $(D_g)_{n+1} = (D_g)_n, \; (h_l)_{n+1} = (h_l)_n$

   $(f^{D_l^s})_{n+1} = \left[1-(D_l^s)_{n+1}\right]^{m((D_l^s)_{n+1})}(Y^{D_l^s})_{n+1} - W_0\exp\left[-\beta(D_l^s)_{n+1}\left(1-(D_l^s)_{n+1}\right)\right] = 0$

   (d) **Unloading and** $\varepsilon_{eff} < \varepsilon_{th}^{h_l}$ **with prior damage:**

   $(D_g)_{n+1} = (D_g)_n,$

   $(h_l)_{n+1} = (h_l)_n + \beta_h\left[(1-(D_g)_{n+1})(1-(h_l)_{n+1})\right]^p, \; (D_l^s)_{n+1} = \frac{(D_l^s)_n(h_l)_n}{(h_l)_{n+1}}$

   (e) **Unloading and** $\varepsilon_{eff} > \varepsilon_{th}^{h_l}$**:**

   $(D_g)_{n+1} = (D_g)_n, \; (h_l)_{n+1} = (h_l)_n, \; (D_l^s)_{n+1} = (D_l^s)_n$

   (f) **Loading and** $(f^{D_g})^{tr} < 0$**:**

   $(D_g)_{n+1} = (D_g)_n, \; (h_l)_{n+1} = (h_l)_n, \; (D_l^s)_{n+1} = (D_l^s)_n$

2. **Update**
   $(\phi_{eff})_{n+1} = (D_g)_{n+1}\left[1-(h_l)_{n+1}\left(1-(D_l^s)_{n+1}\right)\right],$
   $\boldsymbol{\sigma}_{n+1} = \left[1-(\phi_{eff})_{n+1}\right]\boldsymbol{\varepsilon}_{n+1}$
3. **Exit**

$(\partial D_g/\partial\epsilon)$, $(\partial h_l/\partial\epsilon)$, and $(\partial D_l^s/\partial\epsilon)$ to get

$$\left.\begin{aligned}\frac{\partial D_g}{\partial\epsilon} &= \frac{\left[-\frac{DR_2}{Y^{D_g}}\frac{\partial Y^{D_g}}{\partial\epsilon}+\frac{1}{Y^{D_l^s}}\frac{\partial Y^{D_l^s}}{\partial\epsilon}\frac{1}{Y^{D_g}}\frac{\partial Y^{D_g}}{\partial D_l^s}\right]}{\kappa}\\ \frac{\partial D_l^s}{\partial\epsilon} &= \frac{\left[-\frac{1}{Y^{D_l^s}}\frac{\partial Y^{D_l^s}}{\partial\epsilon}\left(DR-\frac{A}{Y^{D_g}}\left[\frac{\partial Y^{D_g}}{\partial h_l}\right]\right)\right]}{\kappa}\end{aligned}\right\} \tag{21}$$

where

$$\kappa = DR_2\left(DR-\frac{A}{Y^{D_g}}\frac{\partial Y^{D_g}}{\partial h_l}\right)-\left(\frac{1}{Y^{D_l^s}}\frac{\partial Y^{D_l^s}}{\partial D_g}-\frac{A}{Y^{D_l^s}}\frac{\partial Y^{D_l^s}}{\partial h_l}\right)\left(\frac{1}{Y^{D_g}}\frac{\partial Y^{D_g}}{\partial D_l^s}\right) \tag{22}$$

$(\partial h_l/\partial\epsilon)$ is obtained as in Case 2 (Eq. (15)). Eqs. (17), (21), and (22) are substituted in Eqns. (12) and (11) to get algorithmic tangent modulus.

**Case 4:** $h_l$ evolves (unloading/rest), $D_l^s$ updated, keeping *secondary damaged* area constant

$$D_g^s = D_l^s h_l D_g = \text{constant} \Rightarrow \dot{D}_l^s = -\frac{D_l^s D_g \dot{h}_l}{h_l D_g} = -\frac{D_l^s \dot{h}_l}{h_l} \tag{23}$$

The continuous form of $[\partial\sigma/\partial\epsilon]$ is written using Eqn. (4) and $\dot{D}_g = 0$ as

$$\dot{\sigma} = E_0(1-\phi_{eff}) - \dot{\phi}E_0\epsilon = E_0(1-\phi_{eff}) + \dot{h}_l D_g E_0\epsilon \tag{24}$$

The Eqn. (24) is written in incremental form as

$$\Delta\sigma = E_0(1-\phi_{eff})\Delta\epsilon + \Delta h_l D_g E_0\epsilon \Rightarrow$$

$$\Delta\sigma = E_0\left(1-D_g(1-h_l+D_l^s h_l)\right)\Delta\epsilon + \Delta h_l D_g(1-D_l^s)E_0\Delta\epsilon + \Delta h_l D_g E_0\epsilon_n \tag{25}$$

The algorithmic tangent modulus is then approximated as

$$E^T \approx E_0\left(1-D_g(1-h_l+D_l^s h_l)\right) + \Delta h_l D_g(1-D_l^s)E_0 \tag{26}$$

As the healing evolution Eqn. 8 cannot be represented in terms of $\dot{\epsilon}$ or $\dot{\sigma}$, the term $\Delta h_l D_g E_0\epsilon_n$ is neglected to obtain an approximate form of the tangent modulus. This expression is more applicable when damage is significant as $\Delta h_l$ is small when $D_g \rightarrow 1$ .

**Case 5:** Only $D_l^s$ evolves by Eqn. (14) as

$$\frac{\partial D_l^s}{\partial\epsilon} = \frac{\frac{-1}{Y^{D_l^s}}\left(\frac{\partial Y^{D_l^s}}{\partial\epsilon}\right)}{DR_2} \tag{27}$$

The tangent modulus is obtained by Eqns. (11), (12), and (27) as

$$E^T = E_0(1-\phi_{eff}) - \frac{\frac{1}{Y^{D_l^s}}\left(\frac{\partial Y^{D_l^s}}{\partial\epsilon}\right)}{DR_2}E_0 h_l D_g\epsilon \tag{28}$$

Box 5.1 shows the 1D local EDH stress update return mapping algorithm

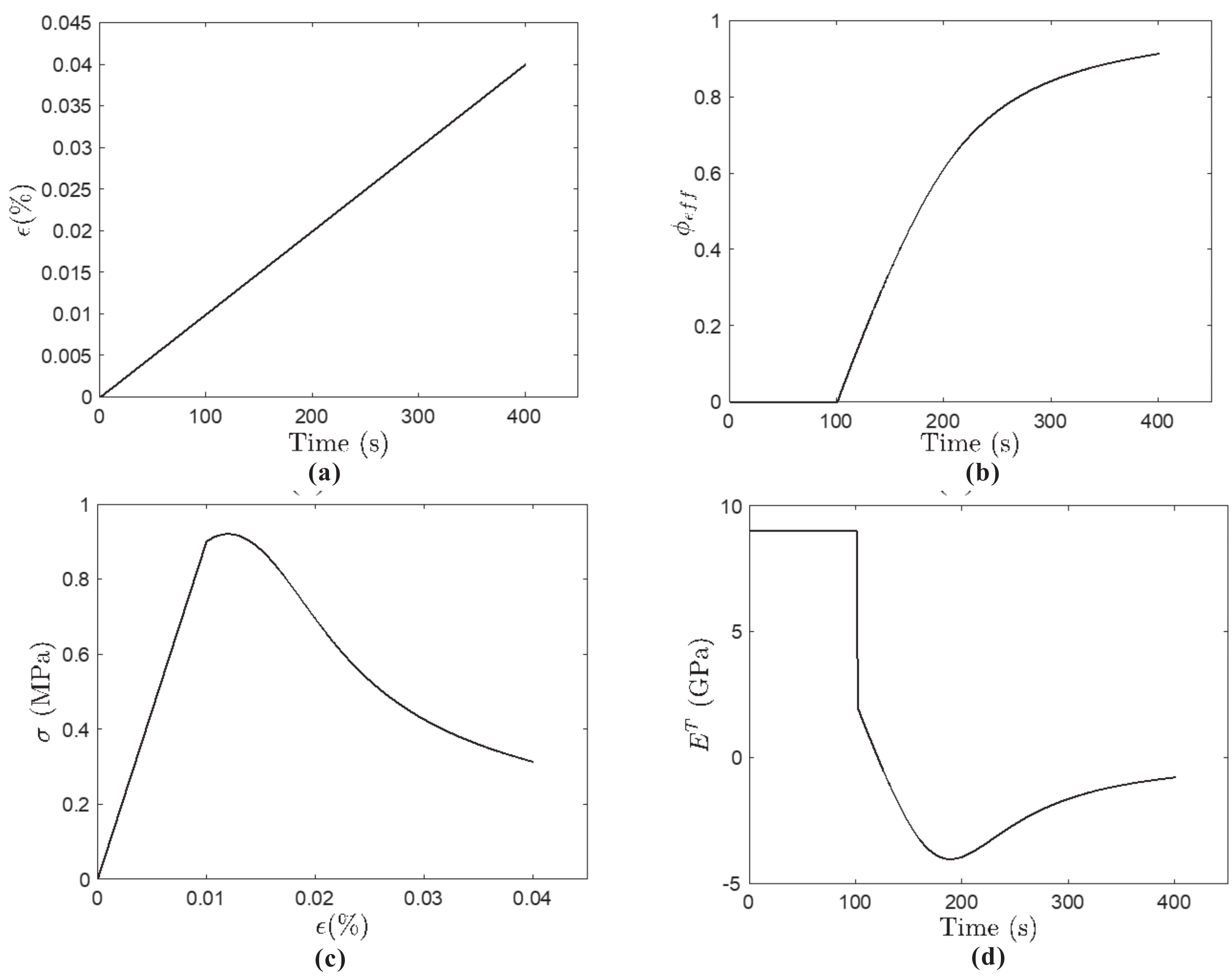


**Figure 1. EDH model applied to monotonic loading: (a) strain input, (b) effective damage, (c) stress vs strain, (d) tangent modulus.**

**Table 1. Input data for elastic damage-healing model**

| Parameter | Value | Parameter | Value | Parameter | Value |
|---|---|---|---|---|---|
| $E$ | 9 GPa | $W_0^{D_g}$ | 1.8 | $\beta_h$ | 0.03 |
| $\beta$ | 0.5 | $p$ | 2 | $\varepsilon_{th}^{h_l}$ | $2.5 \times 10^{-5}$ |
| $m_1$ | 2 | $m_2$ | 1.5 | $m_3$ | 1.1 |
| $W_0^{D_l^s}$ | $0.2W_0^{D_g}$ | | | | |

## 5. RESULTS AND DISCUSSION

The applicability of the proposed EDH model (with and without $D_l^s$) is successfully demonstrated by data in Table 1, simulating different loading cases (Box 5.1).

The model results are also shown with and without the secondary damage variable to explain the significance of $D_l^s$ in capturing the stress-strain response correctly. The input data for the proposed model are listed in Table 1.

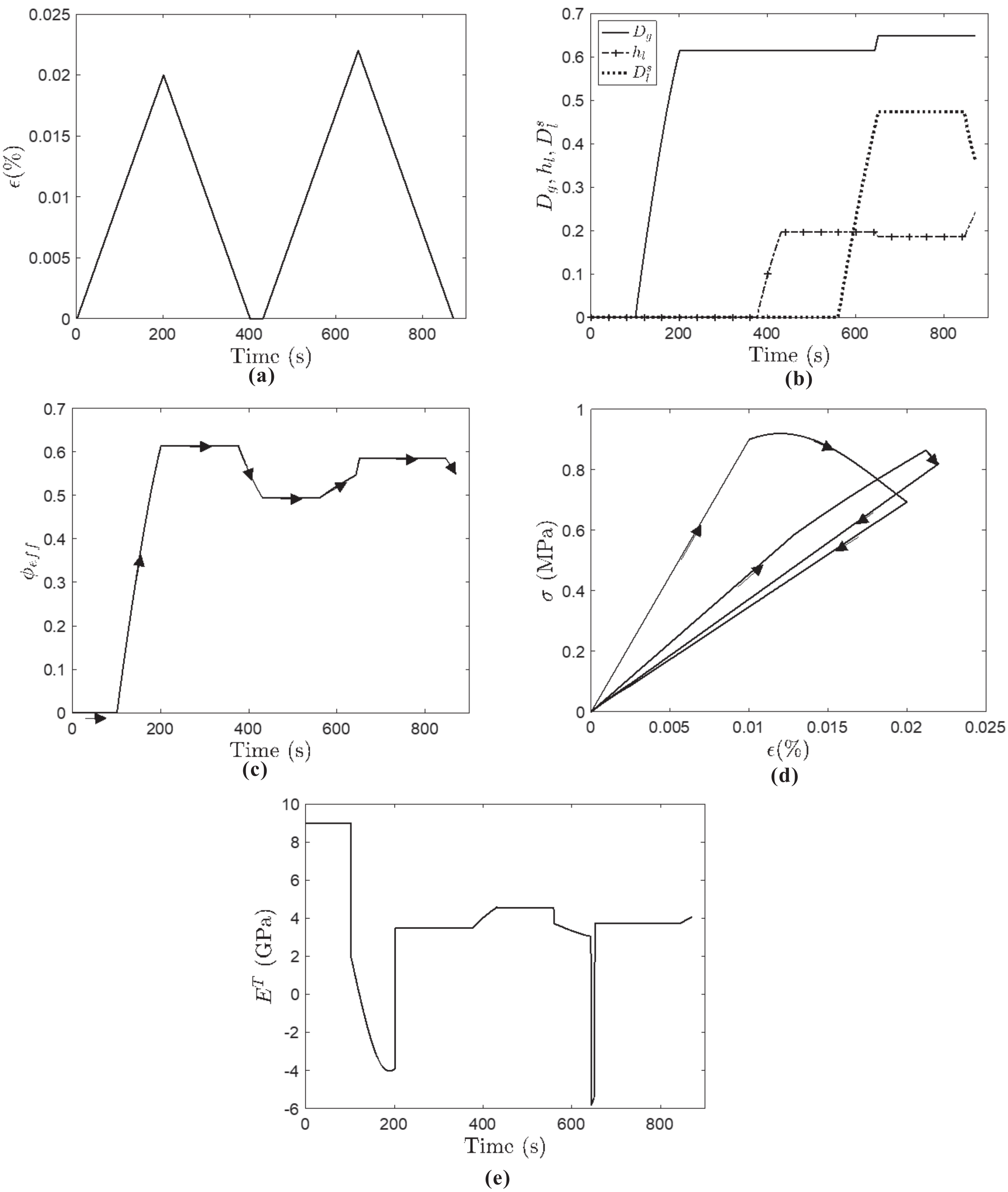


**Figure 2. EDH model with $D_l^s$ applied toloading and unloading strain with rest period: (a) strain input, (b) internal variables, (c) effective damage, (d) stress vs strain, and (e) tangent modulus.**

The response of the EDH model for monotonic loading strain history shown in Figure 1a is first obtained. The primary damage evolution is initiated in this loading process once the threshold energy $W_0^{D_g}$ is exceeded. The effective damage intensity, stress vs strain response and the evolution of tangent modulus are shown in Fig. 1(b)-1(d). There is progressive damage with loading upon initiation, as the material heals when it is unloaded or at rest. The stress-strain response is initially linear, indicating the elastic response and then becomes nonlinear with damage initiation and evolution. The tangent modulus is constant until damage initiation and becomes negative with the change in stress-strain response slope. $E^T$ tends to 0 as damage tends to 1.

The EDH model response is secondly obtained for the unequal unloading strain history shown in Fig. 2(a). The internal variables evolution is shown in Fig. 2(b). Healing evolves when the material is unloaded, and the strain is lesser than a threshold strain (damaged surfaces are closer for healing to occur). Secondary damage evolves during the reloading cycle when the threshold energy $W_0^{D_l^s}$ is exceeded. The secondary damage variable is an area fraction which captures damage in the healed material (refer Eqn. (2)). The monotonic increase requirement is thus not applicable to $D_l^s$ because it is not an absolute variable since $dA_h^D$ may remain constant or change when $D_l^s$ evolves. The variable $D_l^s$ is thus not an independent internal state variable as far as the Helmholtz free energy is concerned.

The apparent decrease in $D_l^s$ in Fig. 2(b) occurs due to healing evolution (increase in $dA_h^D$) in the 800-900 sec. time range (healing evolution during unloading /rest period). It is to be noted that area of healed material that has undergone damage remains unchanged in this time range [$(dA_h^D)^D$remains constant]; the laws of irreversible thermodynamics are thus not violated.

The variable $h_l$ quantifies healing in damaged material (refer to Eqn. (1)). The healed area $dA_h^D$ must remain constant when there is no healing evolution. The slight decrease in $h_l$ in the 600-700 seconds time range is due to primary damage $D_g$ evolution (thus increase in $dA^D$) while the healed area $dA_h^D$ remains constant. An increase in $dA^D$ while $dA_h^D$ remains unchanged results in a decrease in $h_l$. The evolution of internal state variables, $D_g$, $h_l$ and $D_l^s$, must be carefully considered while interpreting the cyclic loading results.

The non-monotonic variation $\phi_{eff}$, combining the influence of $D_g$, $h_l$ and $D_l^s$, is shown in Fig. 2(c). $\phi_{eff}$ increases with damage and decreases with healing. The stress vs strain response is shown in Fig. 2(d), and arrows are marked in Fig. 2(c) and 2(d) to identify the different phases of the stress-strain response and the corresponding $\phi_{eff}$ variation. The stress-strain response slope is higher during reloading than the prior unloading owing to healing evolution. The tangent modulus (shown in Fig. 2(e)) decreases with damage evolution and increases with healing evolution. A negative tangent modulus implies softening in the stress-stain response (negative stress-strain slope).

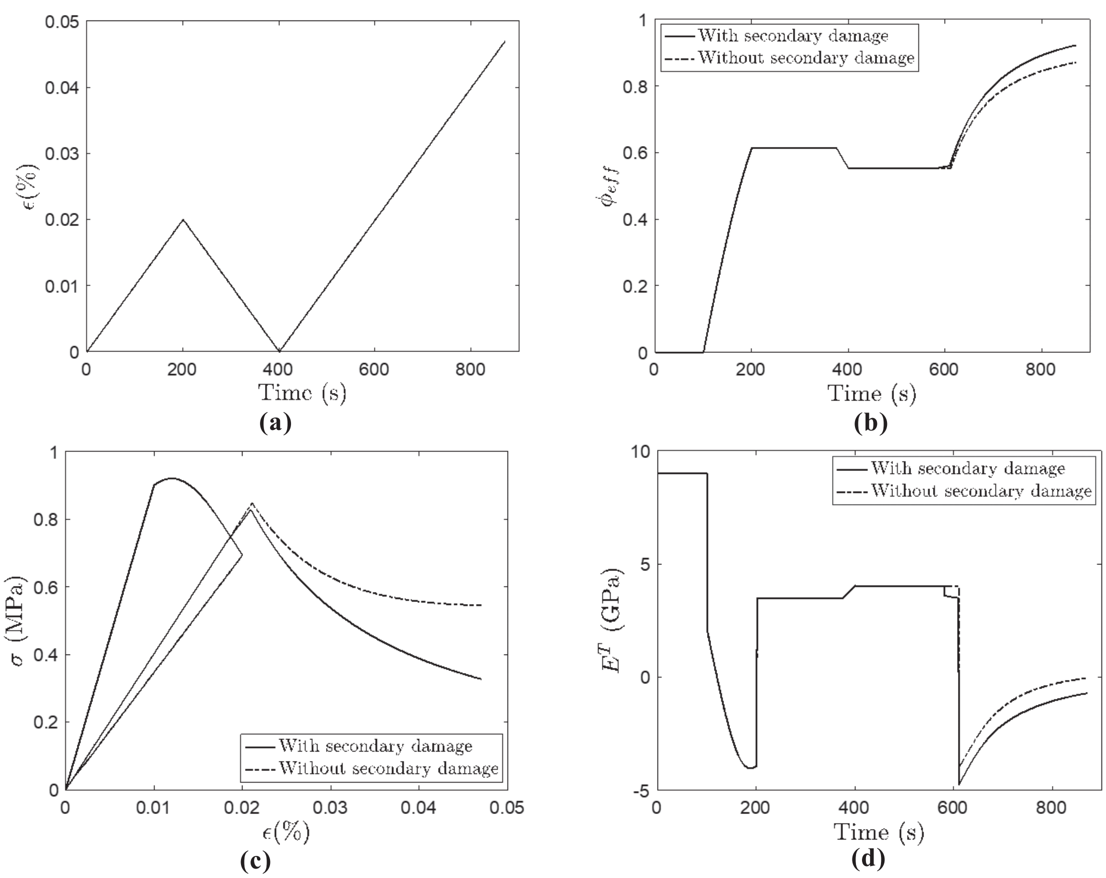


**Figure 3. EDH model (with and without $D_l^s$) applied to loading unloading strain: (a) strain input, (b) effective damage density, (c) stress-strain response, (d) tangent modulus.**

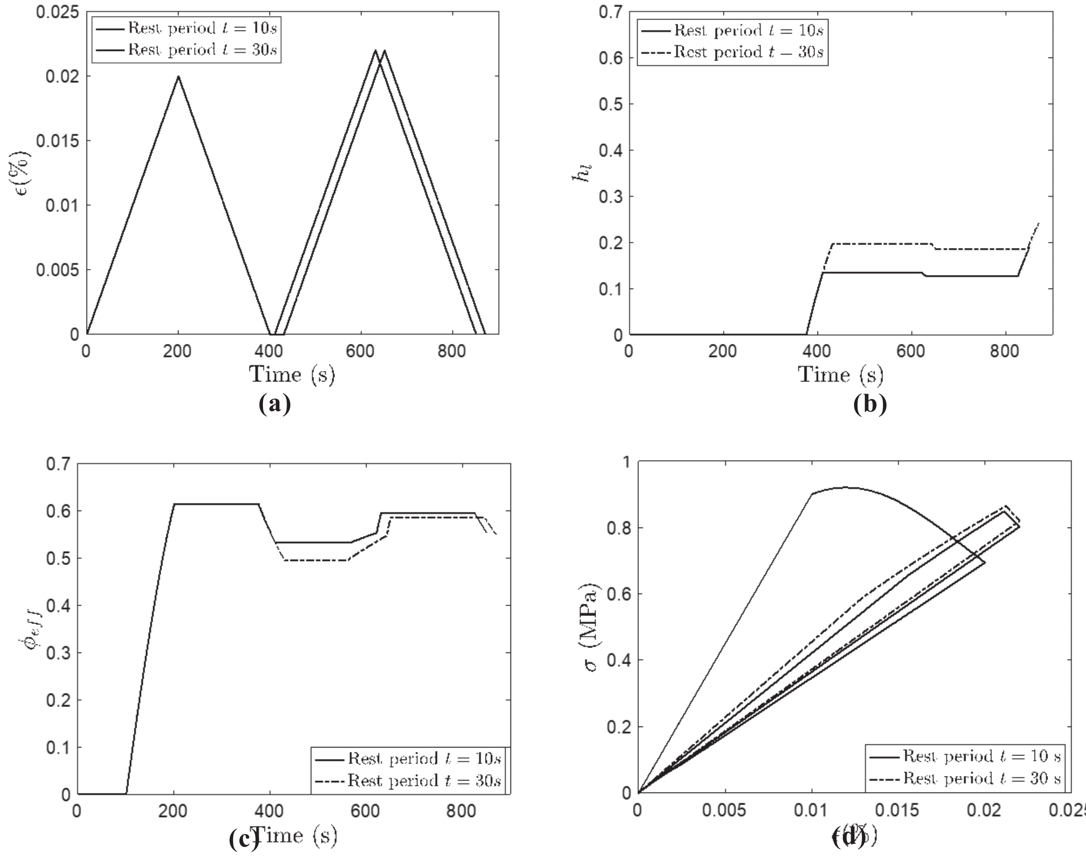


**Figure 4. EDH model (with and without $D_l^s$) applied to equal unloading-reloading strain with rest periods: (a) strain input, (b) healing variable, (c) effective damage density, and (d) stress-strain response.**

The significance of the secondary damage variable is shown in Fig. 3. The EDH model response is shown for the strain history in Fig. 3(a), where the material is loaded, unloaded, and then continuously reloaded. The effective damage density variation, stress-strain response, and tangent modulus variation are shown with and without the secondary damage variable ($D_l^s$) in Fig. 3(b)-3(d). The effective damage is under-predicted without $D_l^s$ as damage in healed material is not captured (Fig. 3(b)). The σ-ϵ response will tend to 0 as $\phi_{eff} \rightarrow 1$ while accounting for healed material damage. The $\sigma - \epsilon$ response without $D_l^s$ starts increasing unrealistically once $\phi_{eff}$ saturates at a value lesser than 1 (healed material remains intact forever). The tangent modulus variation coincides for both cases until the initiation of $D_l^s$ evolution and then diverges.

The effect of the rest period on the material response is demonstrated through strain histories with equal unloading-reloading but different rest periods, as shown in Fig. 4(a). The increase in rest period causes higher healing, as shown in Fig. 4(b). The corresponding $\phi_{eff}$ decreases more in the case of a longer rest period, as shown in Fig. 4(c). It can be seen from the stress-strain response, shown in Fig. 4(d), that the material healing at rest causes higher recovery in its stiffness (seen as an increase in tangent modulus and, thereby the stress-strain slope) during reloading.

## 6. CONCLUSIONS

A constitutive model to capture damage-healing response is developed, coupling a new variable to capture damage in materials that can heal when unloaded or put to rest. The elastic strain equivalence hypothesis is adopted to establish the stress-strain relationship in the damage-healing model. The energy-based criteria for damage evolution in virgin and healed material account for the influence of healing. The proposed evolution function for damage in healed material can be easily modified to capture partial stiffness/strength recovery in a self-healing material.

## REFERENCES

1. García, Álvaro. Self-healing of open cracks in asphalt mastic. *Fuel,* 2012*,* **93,** 264-272.
2. Lei, Z.Q.; Xiang, H.P.; Yuan, Y.J.; Rong, M.Z. & Zhang, M.Q. Room-temperature self-healable and remoldable cross-linked polymer based on the dynamic exchange of disulfide bonds. *Chemistry of Materials*, 2014, **26**(6), 2038-2046.
3. Nuur Laila NajwaThajudin; Zainol, Mohd Hafiz & RaaKhimiShuib. Intrinsic room temperature self-healing natural rubber based on metal thiolate ionic network. *Polymer Testing*, 2021,**93**,106975.
4. Darabi, Masoud K.; Abu Al-Rub, Rashid K. & Little, Dallas N. A continuum damage mechanics framework for modeling micro-damage healing. *Int. J. Solids and Struct.*, 2012,**49**(3-4),492–513.
5. Shahsavari, H.; Baghani, M.; Sohrabpour, S. & Naghdabadi, R. Continuum damage-healing constitutive modeling for concrete materials through stress spectral

decomposition. *Int. J. Damage Mech.*, 2016, **25**(6), 900-918.
6. Yihui, Pan; Tian, Fang & Zhong, Zheng. A continuum damage-healing model of healing agents based self-healing materials. *Int. J. Damage Mech.*, 2018, **27**(5), 754-778.
7. Ever J., Barbero; Greco, Fabrizio & Lonetti, Paolo. Continuum damage-healing mechanics with application to self-healing composites. *Int. J. Damage Mech.,* 2005,**14**(1), 51-81.
8. George Z., Voyiadjis; Shojaei, Amir & Li., Guoqiang. A generalized coupled viscoplastic–viscodamage–viscohealing theory for glassy polymers. *Int. J. Plasticity,* 2012, **28**(1)*,* 21-45.
9. Voyiadjis, George Z., Amir Shojaei, and Guoqiang Li. A thermodynamic consistent damage and healing model for self healing materials. *International Journal of Plasticity,* 2011, **27**(7), 1025-1044.
10. Subramanian, Harini & Mulay, Shantanu S. On the constitutive modelling of elasto-plastic self-healing materials. *Int. J. Solids and Struct.*, 2022, **234**,111289.
11. Subramanian, Harini, and Shantanu S. Mulay. Constitutive modelling of plastically deformable self-healing materials. *Mechanics of Materials, 2022,* **168,** 104272.
12. Subramanian, Harini & Mulay, Shantanu S. Modelling of self-healing in viscoelastic materials. *Int. J. Solids and Struct.,* 2023*,* **270**, 112235.
13. Sathiskumar A., Ponnusami; Krishnasamy, Jayaprakash; Turteltaub, Sergio & Zwaag, Sybrand van der. A cohesive-zone crack healing model for self-healing materials. *Int. J. Solids and Struct.*, 2018, **134**, 249-263.
14. Hehua, Zhu; Zhou, Shuai; Yan, Zhiguo; Woody Ju, J. & Chen, Qing. A two-dimensional micromechanical damage-healing model on microcrack-induced damage for microcapsule-enabled self-healing cementitious composites under tensile loading. *Int. J. Damage Mech.,* 2015, **24**(1), 95-115.
15. Subramanian, Harini & Mulay, Shantanu S. Continuum damage–healing-based constitutive modelling for self-healing materials: application to one-dimensional cyclic loading cases. *Int. J. Adv. Eng. Sci. Appl. Mathematics*. 2020, **12**(1),3–18.
16. Nedjar, Boumediene & Roy, Robert Le. An approach to the modeling of viscoelastic damage application to the long-term creep of gypsum rock materials. *Int. J. Num. Analytical Methods in Geomech*. 2013, **37**(9), 1066–1078.

## CONTRIBUTORS

**Dr Harini Subramanian** is an Assistant Professor in the Department of Mechanical Engineering at IIT Gandhinagar. She obtained her PhD in aerospace engineering from the IIT Madras, Chennai, India. Her research interests include constitutive modelling of materials, continuum damage mechanics, mechanics of composites, and self-healing materials.
Her present work is focused on progressive damage analysis of fibre-reinforced composites and the development of phase field method-based crack propagation models for inelastic materials.

**Dr Shantanu Mulay** is a Professor in the Department of Aerospace Engineering at IIT Madras. He obtained PhD in school of Mechanical and Aerospace Engineering from Nanyang Technological University, Singapore. He also did post-doctoral fellowships, first with Prof. Rohan Abheyaratne (MIT, USA) and second with Prof. Ludovic Noels (ULG, Belgium). He joined Aerospace Engineering Department of IIT Madras, as an Assistant Professor. His research interests include material modelling (composites, viscoelastic-, granular-, and soft materials), continuum damage-healing mechanics, fracture mechanics, and development of numerical meshless methods.